

FULL TITLE

*ASP Conference Series, Vol. **VOLUME**, **YEAR OF PUBLICATION***

NAMES OF EDITORS

Atmospheric Circulation of Hot Jupiters: A Review of Current Understanding

Adam P. Showman

*Department of Planetary Sciences, Lunar and Planetary Laboratory,
University of Arizona, Tucson AZ 85721*

Kristen Menou

Department of Astronomy, 1328 Pupin Hall, Columbia University, New York, NY 10027

James Y-K. Cho

*Astronomy Unit, School of Mathematical Sciences, Queen Mary,
University of London, Mile End Road, London E1 4NS, U.K.*

Abstract. Hot Jupiters are new laboratories for the physics of giant planet atmospheres. Subject to unusual forcing conditions, the circulation regime on these planets may be unlike anything known in the Solar System. Characterizing the atmospheric circulation of hot Jupiters is necessary for reliable interpretation of the multifaceted data currently being collected on these planets. We discuss several fundamental concepts of atmospheric dynamics that are likely central to obtaining a solid understanding of these fascinating atmospheres. A particular effort is made to compare the various modeling approaches employed so far to address this challenging problem.

1. Introduction

An exploding body of observations promises to unveil the meteorology of giant planets around other stars. Because of their high temperatures, short orbital periods, and likelihood of transiting their stars, the hot Jupiters are yielding their secrets most easily, and we now have constraints on radii, composition, albedo, dayside temperature structure, and even day-night temperature distributions for a variety of planets (e.g., Knutson et al. 2007; Cowan et al. 2007; Harrington et al. 2006, 2007; Charbonneau et al. 2002, 2005, 2007; Deming et al. 2005, 2006). A knowledge of atmospheric dynamics is crucial for interpreting these observations.

Understanding the atmospheric circulation of *any* planet is a difficult task, and hot Jupiters are no exception. The difficulty results from the nonlinearity of fluid motion and from the complex interaction between radiation, fluid flow, and cloud microphysics. Turbulence, convection, atmospheric waves, vortices, and jet streams can all interact in a complex manner across a range of temporal and spatial scales. Furthermore, radiative transfer and dynamics are coupled and cannot be understood in isolation. For example, the equator-to-pole temperature contrasts on terrestrial planets depend not only on the rate of latitudinal

energy transport by the circulation but also on the way the atmospheric radiation field is affected by the advected temperature field. Cloud microphysics complicates the problem even more, because the large-scale radiative properties of clouds depend on the microphysics of the cloud particles (particle number density, shape, size distribution, and absorption/scattering properties). We thus have a non-linear, coupled radiation-hydrodynamics problem potentially involving interactions over 14 orders of magnitude, from the cloud-particle scale ($\sim 1 \mu\text{m}$) to the global scale ($\sim 10^8 \text{ m}$ for hot Jupiters).

It is worth emphasizing here the important difference between the complexity of planetary atmospheres and the relative simplicity of stars, exemplified by the main sequence in the HR diagram. While specifying a few global parameters—such as mass, composition, and age—is typically sufficient to understand the key observable properties of stars, this is generally not the case for planetary atmospheres. It is possible that a significant observable diversity exists even among a group of extrasolar planets which share similar global attributes. Understanding such complexity is a challenge for extrasolar planetary science.

A proven method for dealing with the complexity of planetary atmospheres is the concept of a *model hierarchy*. Even a hypothetical computer model that included all relevant processes and perfectly simulated an atmosphere would not, by itself, guarantee an *understanding* of the atmospheric behavior any more than would the observations of the real atmosphere (Held 2005). This is because, in complex numerical simulations, it is often unclear how and why the simulation produces a specific behavior. To discern which processes cause which outcomes, it is important to compare models with a range of complexities (in which various processes are turned on or off) to build a hierarchical understanding.

For example, east-west jet streams occur in the atmospheres of all the planets in our Solar System. The study of these jets involves a wide range of models, all of which have important lessons to teach. The most idealized are pure 2D models that investigate jet formation in the simplest possible context of horizontal, 2D turbulence interacting with planetary rotation (e.g., Williams 1978; Yoden and Yamada 1993; Cho and Polvani 1996b; Huang and Robinson 1998; Sukoriansky et al. 2007). Despite the fact that these simplified models exclude vertical structure, thermodynamics, radiation, and clouds and provide only a crude parameterization of turbulent stirring, they produce jets with several similarities to those on the planets. Next are one-layer “shallow-water-type” models that allow the fluid thickness to vary, which introduces buoyancy waves, alters the vortex interaction lengths, and hence changes the details of jet formation (Cho and Polvani 1996a,b; Scott and Polvani 2007; Showman 2007). 3D models with simplified forcing allow the investigation of jet vertical structure, the interaction of heat transport and jet formation, and the 3D stability of jets to various instabilities (Cho et al. 2001; Williams 1979, 2003; Schneider 2006; Lian and Showman 2007). Such models suggest, for example, that Jupiter and Saturn’s superrotating¹ equatorial jets may require 3D dynamics. Finally are full 3D general-circulation models (GCMs) that include realistic radiative trans-

¹Superrotation is defined simply as a positive (eastward) longitudinally averaged wind velocity at the equator, so that the atmospheric gas rotates faster than the planet.

fer, representations of clouds, and other effects necessary for detailed predictions and comparisons with observations of specific planets. The comparison of simple models with more complex models provides insights not easily obtainable from one type of model alone. This lesson applies equally to hot Jupiters: a hierarchy of models ranging from simple to complex will be necessary to build a robust understanding.

Here we review our current understanding of atmospheric circulation on hot Jupiters. We first describe basic aspects of relevant theory from atmospheric dynamics; this is followed by a detailed comparison of the equations, forcing methods, and results obtained by the different groups attempting to model the atmospheric circulation on these fascinating objects.

2. Basic considerations

Despite the complexity of atmospheric circulation, there exists a 40-year history of work in atmospheric dynamics on solar-system planets that can guide our understanding of hot Jupiters.

Differences between hot Jupiters and solar-system giants: Jupiter, Saturn, Uranus, and Neptune rotate rapidly, with rotation periods ranging from 10 hours (Jupiter) to 17 hours (Uranus). This implies rotationally dominated flows. In contrast, hot Jupiters are expected to rotate synchronously with their orbital periods (Guillot et al. 1996), at least when orbital eccentricity is small, implying rotation periods of 1–5 days for the known transiting planets. Some hot Jupiters will therefore be rotationally dominated, while on others the Coriolis forces will have more modest importance. Note, however, that even “slowly” rotating hot Jupiters rotate much faster than Titan and Venus (rotation periods of 16 and 243 Earth days, respectively). On most hot Jupiters, rotation will have a major impact in modifying the flow geometry.

The forcing on hot Jupiters differs greatly from that on solar-system giants. First is simply the amplitude of the radiative forcing: HD209458b absorbs and reradiates almost $\sim 260,000 \text{ W m}^{-2}$ on a global average, as compared to 240 W m^{-2} for Earth, 14 W m^{-2} for Jupiter, and 0.7 W m^{-2} for Uranus and Neptune. A second difference is that, on the giant planets in our Solar System, the flow seems to be driven by convection, thunderstorms, or baroclinic instabilities with small length scales (see below). Jupiter, Saturn, and Neptune have comparable intrinsic and total heat fluxes, allowing interior convection to greatly affect the atmosphere; the convective zone extends to the visible cloud layers at ~ 1 bar on these planets. For hot Jupiters, however, a statically stable radiative zone extends to pressures of 100–1000 bars, separating the observable atmosphere from the convective interior; furthermore, the interior convective forcing is 10^4 times weaker than the stellar insolation. Thus, the hemispheric-scale stellar forcing is likely to be more dominant on hot Jupiters than for the giant planets in our Solar System. Finally, the expected radiative times above the photospheres on hot Jupiters are extremely short — days or less — whereas those on solar-system giants are years to decades. All these differences will impact the flow in ways that remain to be understood.

Despite our ability to list these differences in forcing, the way the circulation responds to these differences is often subtle. The planets in our Solar System

demonstrate that the relationship between forcing and response is nontrivial. For example, Neptune and Uranus exhibit similar wind patterns but their forcings differ greatly. Neptune's intrinsic heat flux is 1.6 times the absorbed sunlight, implying a strong role for interior convection; on Uranus, in contrast, the intrinsic flux is < 10% of the total flux, implying that external forcing is predominant. Moreover, the small (30°) obliquity on Neptune implies the existence of a regular day-night pattern where the equator receives more sunlight than the poles; in contrast, the 98° obliquity on Uranus means that the poles receive greater sunlight than the equator, and that much of the planet experiences decades of near-continuous sunlight followed by decades of darkness. This Uranus-Neptune comparison suggests that a rotating-stratified atmospheric flow can respond to forcing in a manner which is not simply dictated by the forcing geometry.

Flow length scales: Theoretical work has demonstrated the importance of two fundamental length scales in atmospheric dynamics. First, the *Rhines length*, defined as $(U/\beta)^{1/2}$, is the scale at which planetary rotation causes east-west elongation (jets). Here U is a characteristic horizontal wind speed and $\beta \equiv 2\Omega \cos \phi/a$ is the latitudinal gradient of planetary rotation (Ω is the planetary angular rotation rate, ϕ is the latitude, and a is the planetary radius). Turbulence at small scales tends to be horizontally isotropic, but at length scales approaching the Rhines scale, turbulent structures grow preferentially in the east-west direction rather than the north-south direction. This typically leads to a flow exhibiting a banded structure with east-west jet streams.

Second, the *Rossby deformation radius*, defined as NH/f , is the scale at which pressure perturbations are resisted by the Coriolis forces ($f \equiv 2\Omega \sin \phi$ is the Coriolis parameter, H is the scale height, and N is the Brunt-Väisälä frequency, i.e., the oscillation frequency for a vertically displaced air parcel in a statically stable atmosphere). Vortices often have horizontal sizes near the deformation radius. And baroclinic instabilities — a form of sloping convection that can occur in the presence of horizontal temperature contrasts, converting potential energy to kinetic energy — typically generate turbulent eddies with a horizontal size comparable to the deformation radius. Such instabilities are the primary cause of midlatitude weather on Earth and Mars and may be important in driving the jet streams on Jupiter, Saturn, Uranus, and Neptune (Williams 1979, 2003; Friedson and Ingersoll 1987; Lian and Showman 2007).

On Jupiter and Saturn, the deformation radius and Rhines length are, respectively, ~ 2000 and $\sim 10,000$ km (i.e., much less than the planetary radius). This explains why these planets have narrow jets, numerous cloud bands, and small vortices. On most planets, including Earth's atmosphere, Earth's oceans, and the atmospheres on Mars, Jupiter, and Saturn, there exists a large population of flow structures with sizes near the deformation radius.

In contrast, most hot Jupiters have modest rotation rates, large scale heights (up to ten times that on solar-system giants as a result of the high temperature), and strong vertical stratification (a result of the dominant external irradiation). This means that, on most hot Jupiters, the Rhines length and Rossby deformation radius are close to the planetary radius. Unlike Jupiter and Saturn, the dominant flow structures on hot Jupiters should therefore be planetary in scale (Showman and Guillot 2002; Menou et al. 2003).

The length scales discussed here will strongly influence the atmospheric energetics. In a 3D turbulent fluid, vortex stretching occurs readily, generating small-scale flow structures from large-scale ones and causing energy to cascade downscale. In a quasi-2D fluid such as an atmosphere, however, vortex stretching is inhibited, and energy instead experiences an *inverse cascade* that transfers energy from small to large length scales (Pedlosky 1987; Vallis 2006). (The simplest example is vortex merger, which gradually produces larger and larger vortices over time.) The extent to which the inverse cascade occurs depends on the length scale of energy injection relative to the planetary size: if energy injection occurs at small scales (as may be the case on Jupiter and Saturn), the inverse cascade occurs readily. On the other hand, if energy injection occurs at planetary scales (as may occur on hot Jupiters), the inverse cascade could be less dominant (but see §3.2 below).

Wind speeds: Despite progress, there is still no general theory for what sets the wind speeds on the giant planets in our Solar System. The speeds on all four giants exceed those on Earth, which presumably relates to the lack of a surface (and its associated friction) on the giant planets. More puzzling is the observation that the wind speeds on Neptune exceed those on Jupiter despite the fact that Neptune's total atmospheric heat flux — which ultimately drives the circulation — is only 4% of that on Jupiter. A lesson is that the mean speed involves an equilibrium between *forcing* and *damping* (e.g., friction). Fast winds can occur with weak forcing if the damping is also weak; alternatively, slow winds can occur in the presence of strong forcing if the damping is strong. The damping mechanisms on solar-system giants (which include turbulent mixing and radiative cooling to space) seem to be relatively weak, leading to fast winds. However, it is not fully understood how these mechanisms translate into the hot Jupiter context, particularly since the strength of the damping (as well as the forcing) depends nonlinearly on the flow itself. Careful theoretical work can shed light on how damping and forcing interact to produce an equilibrated flow speed relevant for hot Jupiters.

Despite the above caveats, the known dynamical link between winds and temperatures can be invoked to make useful statements about the winds. In rotating atmospheres, horizontal temperature contrasts are linked to vertical differences in horizontal wind via the *thermal-wind relation* (Holton 2004). (This is often defined in the context of geostrophic balance but it can be extended to a more general balance.) On terrestrial planets, the speed is zero at the surface. So, given an estimate of the equator-to-pole temperature difference, the thermal-wind relation can provide a crude estimate of the actual wind speeds. The forcing and damping processes are relatively well understood for terrestrial planets, and fully nonlinear 3D circulation models do a reasonably good job of simulating the structure and speeds of the winds.

For giant planets, one can profitably apply the thermal-wind relation to obtain the difference in horizontal wind speed between (say) the cloud deck and the base of the weather layer (thought to be at ~ 10 bars for Jupiter) (e.g., Ingersoll and Cuzzi 1969). The difficulty on giant planets is that, unlike the terrestrial planets, the speed at the base of this layer is not necessarily zero —

the planet may exhibit a so-called “barotropic”² wind that penetrates through the convective molecular envelope. In this case, the total wind at the cloud tops would be the sum of the thermal-wind (or “baroclinic” component) and the barotropic wind.

In the context of hot Jupiters, several numerical simulations have been performed that are driven by the intense dayside heating and nightside cooling (Showman and Guillot 2002; Cooper and Showman 2005, 2006; Dobbs-Dixon and Lin 2007; Langton and Laughlin 2007). These simulations are effectively constraining the thermal-wind component of the flow (the height-variable component that exists in the radiative zone above ~ 100 –1000 bars). All of these simulations obtain wind speeds of $\sim 1 \text{ km sec}^{-1}$, in agreement with order-of-magnitude estimates using the thermal-wind relation (Showman and Guillot 2002). All of the published simulations assume that the deep barotropic wind component is zero. It is worth bearing in mind, however, that the barotropic wind component is unknown, and if it is strong then the actual wind speed could differ in magnitude and geometry from that suggested by these simulations. Detailed comparisons of simulations with observed lightcurves and spectra of hot Jupiters can provide constraints on the extent to which the models are capturing the correct flow regime.

Temperatures: Insight into temperature patterns may be gained with timescale arguments. Suppose τ_{rad} is the radiative timescale (i.e., the time for radiation to induce large changes in the entropy) and τ_{advect} is the timescale for air to advect across a hemisphere (e.g., time for air to travel from dayside to nightside or equator to pole). If $\tau_{\text{rad}} \ll \tau_{\text{advect}}$, then large temperature contrasts are expected, whereas if $\tau_{\text{rad}} \gg \tau_{\text{advect}}$, then temperatures should be horizontally homogenized.

To illustrate the usefulness of these arguments, Table 1 lists these timescales and temperature contrasts for the tropospheres of the terrestrial planets. The numbers show general agreement with the above arguments. The radiative time constants are long on Venus, intermediate on Earth, and short on Mars. Regarding transport, we must distinguish longitude from latitude. On Earth and Mars, the planetary rotation dominates the transport of air parcels in longitude, so parcels cycle between day and night with a timescale of 1 day. Venus rotates slowly, but winds and rotation nevertheless transport air from dayside to nightside over a period of days to months. The numbers in the Table imply that $\tau_{\text{rad}} \gg \tau_{\text{advect,lon}}$ for Venus and Earth; in agreement, longitudinal temperature variations are small on these two planets. (They reach $\sim 10 \text{ K}$ on Earth, but this results largely from the uneven continent-ocean distribution; a continent-free “aquaplanet” Earth would exhibit even smaller longitudinal temperature variations.) Latitudinal transport timescales (Table 1) imply that $\tau_{\text{rad}} > \tau_{\text{advect,lat}}$ for Venus, $\tau_{\text{rad}} \sim \tau_{\text{advect,lat}}$ for Earth, and $\tau_{\text{rad}} < \tau_{\text{advect,lat}}$ for Mars. In qualitative

²A barotropic fluid is one where the contours of constant pressure and density align, while a baroclinic fluid is one where these contours misalign. The convective interior has nearly constant entropy and is hence barotropic. Under sufficiently rapid rotation this leads to the Taylor-Proudman theorem in the convective interior, which states that east-west wind is constant in columns that penetrate the molecular envelope in the direction parallel to the rotation axis. This is called a barotropic wind.

agreement with expectations, equator-to-pole temperature contrasts are small on Venus, intermediate on Earth, and large on Mars (Table 1).

Table 1. Timescales and temperature contrasts on terrestrial planets

Planet	τ_{rad}	$\tau_{\text{advect,lon}}$	ΔT_{lon}	$\tau_{\text{advect,lat}}$	ΔT_{lat}
Venus	years	days	<few K	months?	few K
Earth	weeks–months	1 day	~ 10 K	weeks	20–40 K
Mars	days	1 day	~ 20–40 K	days–weeks	~ 50–80 K

Values refer to tropospheres (0.005 bars for Mars, 1 bar for Earth, and ~ 10 bars on Venus). In this table, “day” refers to Earth day (86400 sec). Refs: Gierasch et al. (1997); Peixoto and Oort (1992); Read and Lewis (2004).

What about giant planets? The four solar-system giants exhibit latitudinal temperature contrasts above the clouds of only ~ 5 K (Ingersoll 1990). This results from several processes. First, in the interiors, convective mixing times are short (~decades) but the radiative timescales are geological, so the interior entropy is homogenized (Ingersoll and Porco 1978). On Jupiter, Saturn, and Neptune (which have internal convective heat fluxes comparable to the absorbed solar flux), the top of the constant-entropy interior is close to the photosphere; thus, we expect nearly constant photospheric temperatures across the planet. Second, on all four giants, the radiative timescales above the clouds are long (years to decades), and so even relatively sluggish circulations are capable of homogenizing the temperature patterns. The latter mechanism may be particularly important on Uranus, which lacks a significant interior heat flux.

Hot Jupiters differ from solar-system giants because the radiative timescales above the photosphere are short and because the homogenized interior is hidden below a radiative zone extending to ~ 100–1000 bars (Guillot et al. 1996; Guillot and Showman 2002; Bodenheimer et al. 2001, 2003; Baraffe et al. 2003; Chabrier et al. 2004; Iro et al. 2005), which is far below the expected photosphere pressure of ~ 0.01–1 bar. Large day-night temperature differences are therefore possible at the photosphere depending on τ_{rad} and τ_{advect} there. Current estimates, which derive from radiative calculations that neglect circulation, suggest that τ_{rad} is extremely pressure dependent, ranging from ~ 1 hour at 10^{-3} bars to ~ 1 year at 10 bars (Iro et al. 2005). Considering wind speeds ranging from $0.3\text{--}3\text{ km sec}^{-1}$ then implies that $\tau_{\text{rad}} \sim \tau_{\text{advect}}$ at pressures of ~ 0.1–1 bar. Above this level, day-night temperature differences should be large, while below this level the temperature differences could become small (Showman and Guillot 2002).

A major caveat, of course, is that one must have knowledge of the circulation to estimate τ_{advect} . Even τ_{rad} can depend on the circulation through its dependence on temperature and composition (which in turn depend on the circulation). In the absence of other information, the above arguments are thus generally insufficient to make rigorous predictions of temperature contrasts on planets, since independent timescales are assigned to radiation and hydrodynamics while the two processes are in fact intimately coupled, as mentioned earlier. Nevertheless, the arguments can be used *a posteriori* to understand the temperature patterns occurring in observations — or in detailed nonlinear numerical

simulations of the circulation — when these observations and/or simulations are sufficient to define τ_{advect} and τ_{rad} .

3. Models of atmospheric circulation on hot Jupiters: Similarities and differences

A variety of approaches have been used to study the atmospheric circulation on hot Jupiters. These include solutions of the global two-dimensional shallow-water equations on a rotating sphere (Langton and Laughlin 2007), the global three-dimensional primitive equations³ on a rotating sphere (Showman and Guillot 2002; Cooper and Showman 2005, 2006), the global equivalent-barotropic formulation of these primitive equations on the rotating sphere (Cho et al. 2003, 2007), the two-dimensional Navier-Stokes equations neglecting rotation in an equatorial cross section (Burkert et al. 2005), and the three-dimensional Navier-Stokes equations omitting the polar regions of a rotating sphere (Dobbs-Dixon and Lin 2007). The forcing in all of these models is simplified; no models yet include realistic radiative transfer.

3.1. Work of Showman, Cooper and collaborators

Showman and Guillot (2002), Cooper and Showman (2005), and Cooper and Showman (2006) solved the 3D primitive equations on the whole sphere for parameters relevant to HD209458b. The 3D approach is motivated by the expectation that the radiative time constant varies by orders of magnitude in the vertical (Iro et al. 2005), which in the presence of the day-night heating gradient would cause patterns of temperature and wind that vary both vertically and horizontally in an inherently 3D manner.

The primitive equations are the relevant equations for large-scale flow in statically stable atmospheres whose horizontal dimensions greatly exceed the vertical dimensions. This is expected to be true on hot Jupiters, which have horizontal scales of 10^7 – 10^8 m but atmospheric scale heights of only 200–500 km (depending on temperature and gravity), leading to a horizontal:vertical aspect ratio of 20–500. This large aspect ratio allows the vertical momentum equation to be replaced with local hydrostatic balance, meaning that the *local* vertical pressure gradient $\partial p / \partial z$ is balanced by the local fluid weight ρg , where p , ρ , g , and z are pressure, density, gravity, and height (see for example the derivation in Holton 2004, and §3.5 below). Lateral and height variations in these quantities can still occur and evolve dynamically with the flow. The primitive equations admit the full range of balanced motions, gravity (i.e. buoyancy) waves, rotationally modified (e.g., Rossby and Kelvin) waves, and horizontally propagating sound waves, but they filter out vertically propagating sound waves.

Showman and Guillot (2002), Cooper and Showman (2005), and Cooper and Showman (2006) forced the flow using a Newtonian heating/cooling scheme, which parameterizes the thermodynamic heating rate as $(T_{\text{eq}} - T) / \tau_{\text{rad}}$, where T_{eq} is the specified radiative-equilibrium temperature profile (hot on the dayside, cold on

³The leading-order dynamical equations solved in meteorology and climate studies are called the primitive equations (e.g., Holton 2004); see §3.1 and §3.5.

the nightside), T is the actual temperature, and τ_{rad} is the radiative-equilibrium timescale (a function of pressure). The vertical structure of T_{eq} and τ_{rad} were taken from Iro et al. (2005); the day-night difference T_{eq} was a free parameter that was varied from 100 to 1000 K. This formulation, of course, does not represent a rigorous treatment of radiative transfer, but it provides a physically motivated means to investigate how the expected day-night thermal forcing would drive the atmospheric circulation.

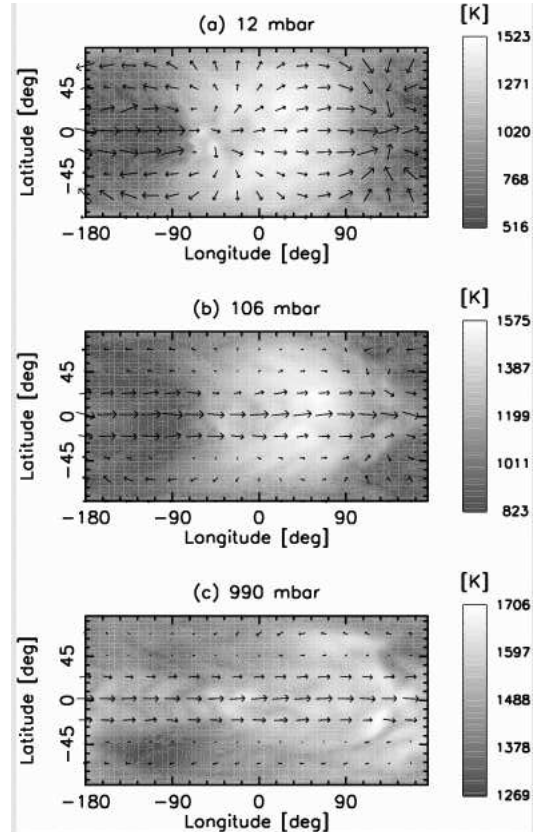


Figure 1. Simulated temperature (greyscale) and horizontal winds (arrows) for three pressure levels from Cooper and Showman (2006). Planetary parameters of HD209458b were adopted.

Figure 1 shows the temperature (greyscale) and winds (arrows) for three layers (10, 100, and 1000 mbar from top to bottom, respectively) after a simulated time of 1000 Earth days for a case with an assumed day-night difference in T_{eq} of 1000 K. The imposed heating contrast leads to winds of several km sec^{-1} , and the day-night temperature contrasts reach 500 K or more. The flow structure has a strongly 3D character. At the top (pressures less than ~ 100 mbar), the radiative time constant is shorter than the time for winds to advect the flow, and the temperature pattern tracks the heating — hot on the day side and cold on the night side — despite the fast winds. At greater pressure, however, the radiative time constant is longer, and dynamics blows the hottest region

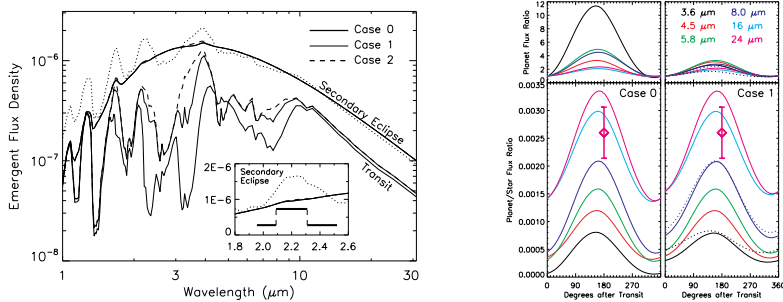


Figure 2. Theoretical infrared spectra (left) and lightcurves in Spitzer IRAC and MIPS bands (right) as calculated by Fortney et al. (2006) from the 3D simulations of Cooper and Showman (2006) for HD209458b. The dayside and nightside spectra (labelled “secondary eclipse” and “transit”, respectively) differ greatly due to the distinct vertical temperature-pressure structures in each region. Case 0, 1, and 2 refer to different assumptions about the chemistry. In the lightcurves, note the phase shift of the peak flux from the time near secondary eclipse (at 180°). See Fortney et al. (2006).

of the atmosphere downwind from the substellar point by 20–60° of longitude depending on altitude. In agreement with the Rhines-length and deformation-radius arguments presented in §2, the simulations exhibit only a small number of broad jets. Interestingly, the development of a superrotating (eastward) equatorial jet is a robust feature in all the simulations of Showman and Guillot (2002), Cooper and Showman (2005), and Cooper and Showman (2006). The mechanism for driving the jet seems to involve equatorward pumping of eddy momentum that occurs in conjunction with the longitudinally varying heating. This process has previously been observed in simplified two-layer models from the Earth sciences (Suarez and Duffy 1992; Saravanan 1993).

By pushing the temperature pattern far from radiative equilibrium, the circulation has major implications for the infrared lightcurves and spectra. Using a two-stream plane-parallel radiative-transfer code, Fortney et al. (2006) calculated infrared lightcurves from the 3D temperature patterns of Cooper and Showman (2005, 2006). These calculations predict that the peak IR emission leads the secondary eclipse by ~ 2 –3 hours in most Spitzer IRAC bands (Fig. 2). This results from advection of the temperature field by the dynamics, which displaces the hottest regions to the east of the substellar point (Fig. 1). Intriguingly, the predicted offset in the flux peak is similar to that in the observed lightcurve for HD189733b, but the simulations overpredict the day-night flux difference and fail to produce a cold region to the west of the antistellar point (Knutson et al. 2007).

The dynamics also drives the vertical temperature profile far from radiative equilibrium. As air advects from nightside to dayside in these simulations, the air aloft warms faster than air at depth (because of shorter radiative time constants aloft), producing a quasi-isothermal region on the dayside despite the absence of such a feature in pure radiative-equilibrium models. This leads to dayside and nightside spectra (Fig. 2, left) that differ substantially from the predictions

of 1D radiative-equilibrium models (Burrows et al. 2005; Barman et al. 2005; Seager et al. 2005; Fortney et al. 2005).

3.2. Work of Cho, Menou and collaborators

In geophysical fluid dynamics, an important distinction is made between flows that are fundamentally 3D and flows whose essence is largely 2D (and hence can be captured in a 2D model), even though they are of course occurring in a 3D atmosphere. For example, the Earth's midlatitude troposphere experiences baroclinic instability, which is a fundamentally 3D process and requires a 3D model to capture. Large parts of the Earth's stratosphere (the region overlying the troposphere), on the other hand, lack baroclinic instabilities because of the strong static stability. Many aspects of the stratosphere—such as the dynamics of the polar vortex, Rossby wave breaking, and turbulent mixing—have been modeled to great advantage with 2D or quasi-2D models (Juckes and McIntyre 1987; Juckes 1989; Polvani et al. 1995). Because of their strong static stabilities and large Rossby deformation radii (which tend to discourage baroclinic instabilities), Cho et al. (2003, 2007) and Menou et al. (2003) have proposed that the basic flow regime of hot Jupiter atmospheres may likewise be successfully captured in a quasi-2D, one-layer formulation.

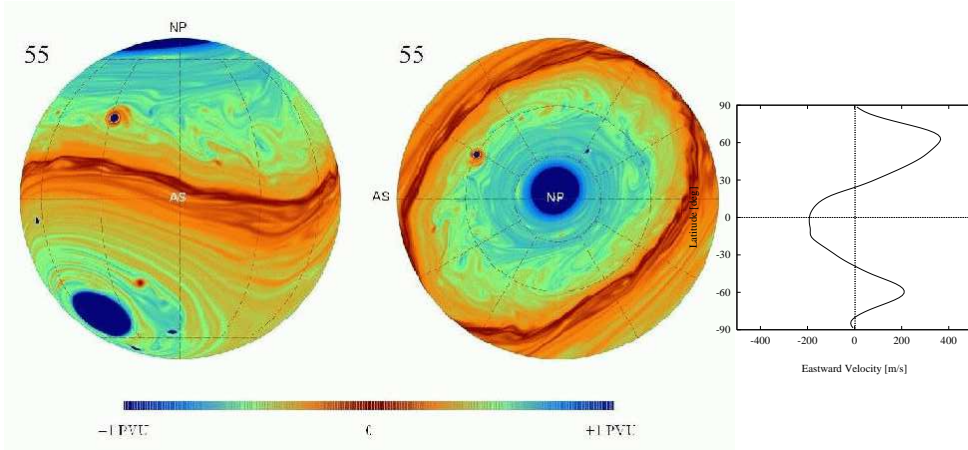


Figure 3. [Left] Equatorial and polar views of potential vorticity (a flow tracer) in a specific hot Jupiter model from Cho et al. (2003, 2007). Note the prominent circumpolar vortices formed as a result of potential vorticity conservation. [Right] Corresponding zonally averaged wind profile, characterized by a small number of broad jets (three in this case).

Adopting this point of view, Cho et al. (2003, 2007) solved the equivalent-barotropic formulation of the primitive equations on the rotating sphere. These equations are a one-layer version of the primitive equations and can formally be obtained by integrating the primitive equations vertically. The vertical integration leads to equations for the column-integrated horizontal velocity, layer thickness, and mean temperature as a function of longitude, latitude, and time. The advantage of this approach is that, by reducing the vertical resolution,

high horizontal resolution can be achieved, allowing numerical solutions to resolve small-scale turbulent interactions that are difficult to capture in a full 3D model. These equations (and the formally related shallow-water equations) are well-suited to the study of two-dimensional jets, vortices, and horizontally propagating gravity and Rossby waves. These simplified equations have a venerable history of successful use in studying dynamical processes in the planetary and atmospheric sciences (for a review see Vasavada and Showman 2005). On the other hand, the full three-dimensional nature of the flow is not represented. These equations exclude 3D processes such as baroclinic instability, vortex tilting, and vertical wave propagation.

Rather than exciting the flow only with a day-night heating contrast, Cho et al. (2003, 2007) also initialize their simulations with small-scale turbulent stirring. Their flows subsequently evolve to states containing meandering polar vortices, breaking Rossby waves, and turbulent mixing (Fig. 3). One may question the relevance of small-scale initialization for hot Jupiter atmospheres, since they are intensely heated on large, hemispheric scales. In considering this question, however, one should remember that coupling between small and large scales in nonlinear flow is a delicate, and still not completely understood, issue. As an example, consider once again Uranus: it is dominantly forced by insolation on a hemispheric scale and yet the rotationally constrained flow is clearly *not* a simple reflection of this external forcing. It is significant that equivalent-barotropic simulations with small-scale initial turbulence are able to reproduce the dominant features of Uranus' atmospheric flow (Cho et al. 2007). Such simulations demonstrate that regardless of the type and scale of forcing, rotation plays a dominant role in shaping the large-scale flows on planets.

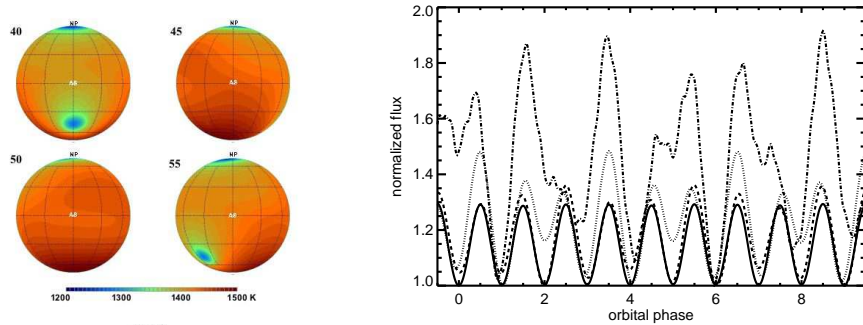


Fig. 3

Figure 4. [Left] Equatorial views of four successive temperature maps for the same model as shown in Fig. 3. Large-scale moving atmospheric features, in particular circumpolar vortices, may lead to significant observable variability. [Right] Examples of thermal infrared phase curves according to the models of Cho et al. (2007). From top to bottom, curves for adopted mean wind speeds of 800, 400, 200 and 100 m/s are shown. At higher wind speeds, contributions from coherent moving atmospheric features become apparent, shifting and deforming the phase curves away from a regular shape (Rauscher et al. 2008).

It is important to realize that the flow is stirred only at the start of the simulations in Cho et al. (2003, 2007). The resulting flow in these dynamically initialized studies can be extremely time-variable, especially when the mean winds in the turbulent initial condition are strong. If such a behavior occurs on a hot Jupiter, then substantial variability in the secondary eclipse depths of a transiting hot Jupiter may be expected (Rauscher et al. 2007b). In addition, signatures of large-scale moving atmospheric features may become apparent (Fig. 4) in the thermal infrared phase curves of these objects (Rauscher et al. 2008). In agreement with Rhines-length and deformation-radius arguments (Showman and Guillot 2002; Cho et al. 2003; Menou et al. 2003) and numerical simulations by Showman and Guillot (2002) and Cooper and Showman (2005, 2006), the flow usually consists of a small number of broad jets (Fig. 3).

3.3. Other work

Langton and Laughlin (2007) performed global numerical simulations of the atmospheric flow on hot Jupiters using the traditional shallow-water equations, which govern the dynamics of a thin layer of hydrostatically balanced, constant-density fluid on a rotating sphere. Mathematically, these equations can be viewed as a special case of the equivalent-barotropic equations in isentropic coordinates when $R/c_p = 1$, where R is the gas constant and c_p is the specific heat at constant pressure (Cho et al. 2007). However, because the density in the shallow-water equations is constant (whereas it is dependent on pressure in the equivalent barotropic equations), the temperature is undefined and there is no thermodynamic energy equation (see Pedlosky 1987, Chapter 3). Note that Eq. 1 of Langton and Laughlin (2007), which they write as an energy equation, is actually the shallow-water mass continuity equation for the layer thickness:

$$\frac{\partial h}{\partial t} + \nabla \cdot (h\mathbf{v}) = 0, \quad (1)$$

where h is layer thickness (a representation of pressure), t is time, and \mathbf{v} is horizontal velocity of the shallow-water layer. Langton and Laughlin (2007) force Eq. 1 by including a Newtonian-relaxation source term $(h_{\text{eq}} - h)/\tau_{\text{rad}}$, where h_{eq} is the equilibrium thickness (thick on dayside, thin on nightside), which adds mass on the dayside and removes it on the nightside. This is a reasonable zeroth-order method to model the effects of radiative cooling on the shallow-water flow (e.g., Polvani et al. 1995; Showman 2007). A rigorous representation of thermodynamic forcing and temperature requires the use of a more general set of equations (such as the equivalent-barotropic, primitive, or compressible Navier-Stokes equations) that, unlike the shallow-water equations, have distinct energy equations. In the planetary context, the shallow-water layer could be interpreted as a thin, stable “weather layer”, possibly overlying a deeper and denser interior. Langton and Laughlin (2007) adopt a radiative time constant of ~ 8 hours, intended to represent conditions expected near the photosphere according to Iro et al. (2005). These forced simulations are initialized from rest.⁴

⁴Langton and Laughlin (2007) also present unforced simulations initialized with small-scale turbulence, similar to the simulations of Cho et al. (2003). In this case, they obtain a flow similar to Cho et al. (2003).

Langton and Laughlin (2007) find that, when the obliquity is assumed zero, their forced flows quickly reach a steady state exhibiting a westward equatorial jet with speeds approaching 1 km sec^{-1} and day-night differences in layer thickness reaching the imposed equilibrium value of $\sim 40\%$. The height field becomes distorted from the equilibrium value, h_{eq} , so that the thickest and thinnest regions are offset from the substellar and antistellar points. Interestingly, despite the development of a westward equatorial jet, these thin and thick regions are displaced to the *east* rather than to the west of the antistellar and substellar points, respectively; the reasons for this phenomenon remain unclear. Langton and Laughlin (2007) also performed simulations with a high obliquity, wherein the starlight alternately heats one hemisphere and then the other; the dynamics here becomes periodic with the orbital period, as expected. In all these simulations, the flow length scales are broad, similar to the previous studies discussed earlier.

Several authors have also performed investigations in limited-area domains. Burkert et al. (2005) perform a 2D study (with coordinates longitude and height) using the Navier-Stokes equations without rotation in a section of an equatorial plane. They parameterize the heating with a flux-limited diffusion scheme using Rosseland mean opacities and an imposed temperature distribution at the top of the model typically ranging from 100 K on the nightside to ~ 1200 K at the substellar point. This scheme induces heating on the dayside and cooling on the nightside. Their standard domain extends 180° in longitude and ~ 6000 km vertically with free-slip wall boundary conditions. Because of the side wall boundary conditions, the flow cannot develop planet-encircling jet streams (as occurs for example in the simulations of Showman and Guillot 2002; Cooper and Showman 2005; Cho et al. 2003, 2007; Dobbs-Dixon and Lin 2007). Instead, an overturning circulation develops with rising motion near one wall, sinking motion near the other, and lateral currents that connect the two. The nominal opacity used for calculating the diffusion coefficients in the radiative scheme is based on that expected for grains in the interstellar medium, although simulations were also performed with opacities ranging from 10^{-3} to 10^2 times the nominal values. The strength of the flow depends on the assumed opacity; in the nominal cases, the wind speeds reach several km sec^{-1} and day-night temperature differences reach ~ 700 K at the expected photosphere pressure.

Dobbs-Dixon and Lin (2007) investigated the atmospheric circulation by solving the 3D Navier-Stokes equations in the low- and mid-latitudes of a rotating sphere (the polar regions were omitted). As in Burkert et al. (2005), they parameterized the radiative-transfer with flux-limited diffusion using Rosseland-mean opacities. In addition to the Coriolis force, they included the centrifugal force in the equation of motion; this differs from the approach taken in most global atmospheric circulation models, which typically account for the gravitational relaxation of the planetary interior to the planetary rotation by absorbing the centrifugal force into the gravity (see Holton 2004, p. 12–13). Similar to Showman and Guillot (2002) and Cooper and Showman (2005, 2006), their simulations develop an eastward jet at the equator and westward jets in midlatitudes. The vertical thickness of these jets varies substantially with longitude. Dobbs-Dixon and Lin (2007) find that the flow strength depends on the assumed opacity, as in Burkert et al. (2005); in their nominal cases, wind speeds reach

several km sec^{-1} and day-night temperature differences at the expected photosphere reach $\sim 700\text{--}800\text{ K}$.

The studies described so far all focus on flow near the photosphere. In contrast, Koskinen et al. (2007) performed 3D simulations of the thermosphere and ionosphere of hot Jupiters using the 3D primitive equations. In their simulations, the domain extended from $\sim 2\text{ }\mu\text{bar}$ to $\sim 0.04\text{ nbar}$ or less. The simulations included molecular heat conduction and diffusion, which are important due to the large molecular mean-free paths at the sub- μbar pressures investigated in this study. Simplified schemes for photochemistry, stellar extreme ultraviolet (EUV) heating, and radiative cooling by H_3^+ were also implemented. The emphasis was on planets from 0.2–1 AU from their stars (in contrast to the other investigations described in this review, which tend to emphasize planets at $< 0.1\text{ AU}$). The simulations developed strong flows of $\sim 1\text{ km sec}^{-1}$ from the substellar point to the antistar point; temperatures often reached 10,000 K or more depending on assumptions about the cooling. The wind, temperature, and chemistry patterns have implications for the rate of atmospheric escape to space.

3.4. Speculations on the causes of model differences

Published simulations of atmospheric circulation on hot Jupiters have similarities as well as differences. Despite the range of approaches, all the published studies agree that the flow on typical hot Jupiters will exhibit only a small number of broad jets, consistent with Rhines scale and deformation radius arguments (Showman and Guillot 2002; Cooper and Showman 2005, 2006; Menou et al. 2003; Cho et al. 2003, 2007; Langton and Laughlin 2007; Dobbs-Dixon and Lin 2007). As discussed earlier, this agreement results from the modest rotation rates, high temperatures, and strong static stabilities of hot-Jupiter atmospheres. (Indeed, this bodes well for characterizing the dynamical state with spectra and lightcurves, which sample globally or near-globally.) Published simulations that attempt to predict the wind speeds also generally agree that the baroclinic component of the flow (i.e., the difference in the flow speeds between the photosphere and the base of the radiative zone) may reach $\sim 1\text{ km sec}^{-1}$ or more (Showman and Guillot 2002; Cooper and Showman 2005, 2006; Burkert et al. 2005; Langton and Laughlin 2007; Dobbs-Dixon and Lin 2007).

On the other hand, the models also exhibit a number of important differences. Characteristic features of the Cho et al. (2003, 2007) simulations include development of large polar vortices, extensive turbulent mixing, and time variability, if the global average wind speed is large and/or the day-night hemispheric temperature difference is weak. In contrast, the simulations of Showman and Guillot (2002), Cooper and Showman (2005, 2006), and Langton and Laughlin (2007) exhibit steadier flow behavior and tend to lack the high degree of turbulent mixing that occurs in the Cho et al. simulations. While differences in model resolution and numerical methods surely contribute, one cause of these differences seems to be the issue of whether the initial flow contains turbulence (as in Cho et al. 2003, 2007), in addition to a global-scale day-night forcing (as in Showman and Guillot 2002; Cooper and Showman 2005, 2006; Langton and Laughlin 2007; Dobbs-Dixon and Lin 2007). Certainly, if the initial condition contains strong, closely-packed vortices (as in Cho et al.), the subsequent process of vortex mergers and planetary wave radiation naturally induces turbulent mixing

and produces, as an end state, a small number of large vortices that typically end up near the poles (see Cho and Polvani 1996b). On the other hand, when the energy source comprises global-scale day-night forcing, the dominant length scales are large (\sim planetary radius), leading to a global-scale flow.⁵

Therefore, a key distinction between the various models published so far has to do with the problem of understanding how the stellar forcing is expressed in the atmospheric flow itself. As we have already commented, this is a subtle issue, even for solar-system giant planets. However, there are good reasons to believe that progress on this issue is possible in the future. First, on the modeling side, detailed schemes to treat the radiative transfer in hot Jupiter atmospheres are being developed, so that more reliable treatments of the non-linear radiation-hydrodynamics involved in expressing this forcing can be implemented. These modeling efforts may thus be able to shed some light as to what the nature of the flow forcing in hot Jupiter atmospheres is. Secondly, observations may provide important guidance for the modelers, as is the case even in solar-system atmospheric studies.⁶ This is particularly true of the issue of atmospheric turbulence. All solar-system atmospheres are turbulent. For hot Jupiters, there is an expectation that the combination of turbulence and large fundamental atmospheric scales may lead to significant variability in various observables. Observations may thus help distinguish a rather steady atmospheric behavior from a more variable one, and in doing so establish a distinction between the two modeling approaches (and associated forcing schemes) discussed above. As has always been the case with solar-system studies, progress in understanding hot Jupiters is likely to involve repeated iterations between observations and modeling.

Another difference in published studies is the development of robust equatorial superrotation in the 3D simulations (Showman and Guillot 2002; Cooper and Showman 2005, 2006; Dobbs-Dixon and Lin 2007), whereas the one-layer calculations produce both westward (i.e., subrotating) and eastward equatorial flow (Cho et al. 2003, 2007; Langton and Laughlin 2007). Regarding the superrotation, the studies by Showman and Guillot (2002) and Cooper and Showman (2005, 2006) involved a range of different assumptions for the initial temperature profile, the day-night equilibrium temperature difference, and the radiative time constants. Some simulations were initialized with a strong *westward* jet to determine if it could be retained in the simulation. Intriguingly, all of these simulations produced a strong eastward jet at the equator. This suggests that the superrotation is a robust phenomenon, at least within the context of the adopted input parameters and forcing approach. More study is needed to understand this phenomenon.

The forcing in all published models is simplified; no models yet include realistic representations of radiative transfer. Burkert et al. (2005) and Dobbs-Dixon and Lin (2007) adopted a diffusion approach, which is accurate in the deep, optically thick atmosphere (and hence is commonly used in the interior portion of evolu-

⁵Large-scale jet streams can exhibit shear instabilities that generate small-scale turbulence, but this phenomenon has not been obviously apparent in the radiatively forced studies performed to date.

⁶Even advanced GCMs, which are treated as much as possible as first-principle models, generally include numerous free parameters which are adjusted to match observed atmospheres.

tion models); however, the radiative transfer is non-diffusive above the photosphere, so this approach loses accuracy in the observable atmosphere (i.e. at and above the photosphere). In contrast, the shallow-water studies of Langton and Laughlin (2007) and the 3D studies of Showman and Guillot (2002) and Cooper and Showman (2005, 2006) adopted a Newtonian heating/cooling scheme. This scheme has enjoyed a long history of successful use in process studies of planetary climate. However, it effectively involves a linearization of the heating rate around the radiative-equilibrium state and neglects the fact that the radiative equilibrium temperature and timescale can depend on the atmosphere's dynamical response, particularly when actual temperatures are far from the prescribed radiative-equilibrium values. Finally, Cho et al. (2003, 2007) did not include radiative forcing at all but instead performed adiabatic simulations driven by a combination of initial turbulence and large-scale pressure deflections. This approach allows an exploration of how the flow behavior depends on the energy (which is a tunable input parameter) and therefore provides a useful baseline. On the other hand, there is no ability to predict mean flow speeds, and the absence of radiative forcing means that these simulations cannot capture aspects of the dynamics that crucially depend on such forcing. The adopted approaches, while simplified, nevertheless all serve the intended purpose of providing plausible sources of energy injection. Inclusion of realistic radiative transfer is an important goal for future modeling work.

Interestingly, infrared lightcurve observations could allow an observational constraint on the wind patterns, at least for planets with a photosphere deep enough for the radiative time to be comparable to the advection time. To varying degrees, the simulations performed to date suggest that dynamics can distort the temperature pattern in a complex manner, so that the temperature field does not simply track the stellar heating pattern (Showman and Guillot 2002; Cooper and Showman 2005, 2006; Cho et al. 2003, 2007; Burkert et al. 2005; Dobbs-Dixon and Lin 2007; Langton and Laughlin 2007). For example, the hottest and coldest regions may be displaced from the substellar and antisubstellar points, respectively, leading to phase shifts in infrared lightcurves relative to that expected without dynamics. While there will likely be degeneracies in interpretation (i.e., multiple flow patterns may explain a given lightcurve), such data will nevertheless provide powerful constraints to distinguish among the various models.

3.5. The validity of hydrostatic balance

A scaling analysis demonstrates that local hydrostatic balance is approximately valid for the large-scale flow on hot Jupiters. It is important to emphasize that the local-hydrostatic-balance assumption in the primitive equations derives from the assumption of large aspect ratio and *not* from any assumption on wind speed. However, the fact that estimated wind speeds on hot Jupiters are several km sec^{-1} , which is close to the 3-km sec^{-1} speed of sound in these atmospheres, suggests that we consider the validity of the primitive equations in the hot-Jupiter context. The full Navier-Stokes vertical momentum equation can be written

$$\frac{\partial w}{\partial t} + \mathbf{v} \cdot \nabla w = -\frac{1}{\rho} \frac{\partial p}{\partial z} - g + 2u\Omega \cos \phi \quad (2)$$

where w is vertical wind speed, t is time, \mathbf{v} is the horizontal wind velocity, and u is the east-west wind speed. The background static hydrostatic balance is irrelevant to atmospheric circulation and can be removed from the equation. Define $p = p_0(z) + p'$ and $\rho = \rho_0(z) + \rho'$ where p_0 and ρ_0 are the time-independent basic-state pressure and density and, by construction, $\partial p_0/\partial z \equiv -\rho_0 g$. Primed quantities are the deviations from this basic state caused by dynamics. Substituting these expressions into Eq. 2, we can rewrite the equation as

$$\frac{\partial w}{\partial t} + \mathbf{v} \cdot \nabla w = -\frac{1}{\rho} \left(\frac{\partial p'}{\partial z} - \rho' g \right) + 2u\Omega \cos \phi \quad (3)$$

where the basic-state hydrostatic balanced has been subtracted off. The terms in parentheses give only the flow-induced contributions to vertical pressure gradient and weight (they go to zero in a static atmosphere).

For local hydrostatic balance to be a reasonable approximation, the terms in parenthesis must be much larger than the other terms in the equation. The magnitude of $\partial w/\partial t$ is approximately w/τ , where τ is a flow evolution timescale, and the magnitude of $\mathbf{v} \cdot \nabla w$ is the greater of uw/L and w^2/H where L is the horizontal flow scale and H is the vertical flow scale. For global-scale flows, $L \sim 10^7\text{--}10^8$ m and $\tau \sim 10^4\text{--}10^5$ sec. The large-scale flow varies vertically over a scale height $H \sim 300$ km (Showman and Guillot 2002; Cooper and Showman 2005, 2006; Dobbs-Dixon and Lin 2007). For the simulated flow regime in Cooper and Showman (2005, 2006) and Dobbs-Dixon and Lin (2007), $\mathbf{v} \sim u \sim 3 \text{ km sec}^{-1}$, $g \sim 10 \text{ m sec}^{-2}$, $\Omega \sim 2 \times 10^{-5} \text{ sec}^{-1}$, and $w \sim 10\text{--}100 \text{ m sec}^{-1}$. With these values, we find that $\partial w/\partial t \leq 10^{-2} \text{ m sec}^{-2}$, $uw/L \leq 0.03 \text{ m sec}^{-2}$, $w^2/H \leq 0.03 \text{ m sec}^{-2}$, and $\Omega u \sim 0.1 \text{ m sec}^{-2}$. In comparison, for a hot Jupiter with day-night temperature differences of several hundred K, the flow-induced hydrostatic terms $\rho'g/\rho$ and $\rho^{-1}\partial p'/\partial z$ are each $\sim 10 \text{ m sec}^{-2}$.

This analysis implies that, for global-scale hot-Jupiter flows, the greatest departure from hydrostaticity results from the vertical Coriolis force, which causes a $\sim 1\%$ deviation from hydrostatic balance. The acceleration terms on the left side of Eq. 3 (which are necessary for vertically propagating sound waves) cause a $\sim 0.3\%$ deviation from hydrostatic balance. Hydrostatic balance is thus a reasonable approximation for the large-scale flow. Nonhydrostatic effects of course become important at small scales, and it is conceivable that these effects interact with the large-scale flow in nontrivial ways. For hot Jupiters, the acceleration terms on the left side of Eq. 3 only become important for structures with vertical or horizontal scales less than ~ 30 km and $\sim 500\text{--}1000$ km, respectively. In a numerical model that solved the full Navier-Stokes equations, the grid resolution would have to be substantially finer than these values for the nonhydrostatic behavior to be accurately represented. A full Navier-Stokes solution with a coarse resolution would effectively be resolving just the global-scale hydrostatic component of the flow.

3.6. The need for model validation

Due to the complexity of processes involved in modeling the coupled radiation-hydrodynamics of a planetary atmosphere, it is customary in the field of geophysical fluid dynamics and atmospheric sciences to implement robust validation schemes for any simulation tool. Typically, both radiative transfer modules and

dynamical cores (i.e., “primitive equation solvers”) are subjected to standard test cases or inter-comparisons aimed at quantifying their performance and accuracy in conserving important quantities, such as energy and enstrophy (“vortical energy”). For example, a classical benchmark test for dynamical cores is the Held-Suarez test, which isolates baroclinic dynamics from radiative transfer issues by using a simple, Newtonian cooling scenario (Held and Suarez 1994).

The issue of model validation is a particularly critical one for hot Jupiter studies. Earth and planetary scientists have access to detailed information on the atmospheres they study, allowing serious model flaws to be rapidly identified. This is not the case with hot Jupiter atmospheres. While information available from observation of these distant atmospheres is rapidly increasing, it still remains subject to degeneracies in interpretation. This is so even if “eclipse maps” eventually become available (Williams et al. 2006; Rauscher et al. 2007a). As a result, rigorous model validations using test cases and Solar System examples will be critical. Successful model validations can be achieved by explicitly reproducing known features in the Solar System planet atmospheres (e.g. Cho et al. 2007), using simulation tools which have been well-tested previously (e.g. Showman and Guillot 2002; Cho et al. 2003; Cooper and Showman 2005) or by designing appropriate inter-comparison tests tailored for hot Jupiter problems.

4. Summary

The study of hot Jupiter atmospheres is maturing. While data of increasing quality are being collected, atmospheric models are also being refined to help build a robust, hierarchical understanding of these unusual atmospheres. Indeed, one of the main motivations for studying these atmospheres, which is also a main source of difficulty, is the unusual physical regime that characterizes them. Hence, hot Jupiters represent new laboratories for studying the complex physics of giant planet atmospheres. In this way, they offer the promise of extending the boundary of comparative planetology well beyond the solar-system planets.

Acknowledgments. We thank the editors for allowing us to write a joint review paper. The preparation of this paper was supported by a NASA Planetary Atmospheres grant to APS and NASA contract NNG06GF55G to KM.

References

Baraffe, I., G. Chabrier, T. S. Barman, F. Allard, and P. H. Hauschildt, 2003: *A&A*, **402**, 701–712.

Barman, T. S., P. H. Hauschildt, and F. Allard, 2005: *ApJ*, **632**, 1132–1139.

Bodenheimer, P., D. N. C. Lin, and R. A. Mardling, 2001: *ApJ*, **548**, 466–472.

Bodenheimer, P., G. Laughlin, and D. N. C. Lin, 2003: *ApJ*, **592**, 555–563.

Burkert, A., D. N. C. Lin, P. H. Bodenheimer, C. A. Jones, and H. W. Yorke, 2005: *ApJ*, **618**, 512–523.

Burrows, A., I. Hubeny, and D. Sudarsky, 2005: *ApJ*, **625**, L135–L138.

Chabrier, G., T. Barman, I. Baraffe, F. Allard, and P. H. Hauschildt, 2004: *ApJ*, **603**, L53–L56.

Charbonneau, D., T. M. Brown, R. W. Noyes, and R. L. Gilliland, 2002: *ApJ*, **568**, 377–384.

Charbonneau, D., T. M. Brown, A. Burrows, and G. Laughlin, 2007: *Protostars and Planets V*, B. Reipurth, D. Jewitt, and K. Keil, Eds., pp. 701–716.

Charbonneau, D., et al., 2005: *ApJ*, **626**, 523–529.

Cho, J. Y.-K., and L. M. Polvani, 1996a: *Science*, **8**(1), 1–12.

Cho, J. Y.-K., and L. M. Polvani, 1996b: *Physics of Fluids*, **8**, 1531–1552.

Cho, J. Y.-K., M. de la Torre Juárez, A. P. Ingersoll, and D. G. Dritschel, 2001: *J. Geophys. Res.*, **106**, 5099–5106.

Cho, J. Y.-K., K. Menou, B. M. S. Hansen, and S. Seager, 2003: *ApJ*, **587**, L117–L120.

Cho, J. Y.-K., K. Menou, B. M. S. Hansen, and S. Seager, 2007: *ApJ*, submitted. arXiv:astro-ph/0607338.

Cooper, C. S., and A. P. Showman, 2005: *ApJ*, **629**, L45–L48.

Cooper, C. S., and A. P. Showman, 2006: *ApJ*, **649**, 1048–1063.

Cowan, N. B., E. Agol, and D. Charbonneau, 2007: *MNRAS*, **379**, 641–646.

Deming, D., S. Seager, L. J. Richardson, and J. Harrington, 2005: *Nat*, **434**, 740–743.

Deming, D., J. Harrington, S. Seager, and L. J. Richardson, 2006: *ApJ*, **644**, 560–564.

Dobbs-Dixon, I., and D. N. C. Lin, 2007: *ApJ*, submitted.

Fortney, J. J., M. S. Marley, K. Lodders, D. Saumon, and R. Freedman, 2005: *ApJ*, **627**, L69–L72.

Fortney, J. J., C. S. Cooper, A. P. Showman, M. S. Marley, and R. S. Freedman, 2006: *ApJ*, **652**, 746–757.

Friedson, J., and A. P. Ingersoll, 1987: *Icarus*, **69**, 135–156.

Gierasch, P. J., et al., 1997: *Venus II: Geology, Geophysics, Atmosphere, and Solar Wind Environment*, S. W. Bougher, D. M. Hunten, and R. J. Philips, Eds., pp. 459–500.

Guillot, T., and A. P. Showman, 2002: *A&A*, **385**, 156–165.

Guillot, T., A. Burrows, W. B. Hubbard, J. I. Lunine, and D. Saumon, 1996: *ApJ*, **459**, L35+.

Harrington, J., B. M. Hansen, S. H. Luszcz, S. Seager, D. Deming, K. Menou, J. Y.-K. Cho, and L. J. Richardson, 2006: *Science*, **314**, 623–626.

Harrington, J., S. Luszcz, S. Seager, D. Deming, and L. J. Richardson, 2007: *Nat*, **447**, 691–693.

Held, I., 2005: *Bull. Amer. Meteorological Soc.*, **86**.

Held, I. M., and M. J. Suarez, 1994: *Bulletin of the American Meteorological Society*, vol. 75, Issue 10, pp. 1825–1830, **75**, 1825–1830.

Holton, J. R., 2004: *An Introduction to Dynamic Meteorology*, 4th Ed.. Academic Press, San Diego.

Huang, H.-P., and W. A. Robinson, 1998: *Journal of Atmospheric Sciences*, **55**, 611–632.

Ingersoll, A. P., 1990: *Science*, **248**, 308–315.

Ingersoll, A. P., and J. N. Cuzzi, 1969: *Journal of Atmospheric Sciences*, **26**, 981–985.

Ingersoll, A. P., and C. C. Porco, 1978: *Icarus*, **35**, 27–43.

Iro, N., B. Bézard, and T. Guillot, 2005: *A&A*, **436**, 719–727.

Juckes, M., 1989: *Journal of Atmospheric Sciences*, **46**, 2934–2956.

Juckes, M. N., and M. E. McIntyre, 1987: *Nat*, **328**, 590–596.

Knutson, H. A., D. Charbonneau, L. E. Allen, J. J. Fortney, E. Agol, N. B. Cowan, A. P. Showman, C. S. Cooper, and S. T. Megeath, 2007: *Nat*, **447**, 183–186.

Koskinen, T. T., A. D. Aylward, C. G. A. Smith, and S. Miller, 2007: *ApJ*, **661**, 515–526.

Langton, J., and G. Laughlin, 2007: *ApJ*, **657**, L113–L116.

Lian, Y., and A. P. Showman, 2007: *Icarus*, submitted.

Menou, K., J. Y.-K. Cho, S. Seager, and B. M. S. Hansen, 2003: *ApJ*, **587**, L113–L116.

Pedlosky, J., 1987: *Geophysical Fluid Dynamics*, 2nd Ed.. Springer-Verlag, New York.

Peixoto, J. P., and A. H. Oort, 1992: *Physics of Climate*. American Institute of Physics, New York.

Polvani, L. M., D. W. Waugh, and R. A. Plumb, 1995: *Journal of Atmospheric Sciences*,

52, 1288–1309.

Rauscher, E., K. Menou, J. Y.-K. Cho, S. Seager, and B. M. S. Hansen, 2007a: *ApJ*, **662**, L115–L118.

Rauscher, E., K. Menou, S. Seager, D. Deming, J. Y.-K. Cho, and B. M. S. Hansen, 2007b: *ApJ*, **664**, 1199–1209.

Rauscher, E., K. Menou, and coauthors, 2008: *ApJ*, in preparation.

Read, P. L., and S. R. Lewis, 2004: *The Martian Climate Revisited*. Springer/Praxis, New York.

Salby, M. L., 1989: *Tellus*, **41A**, 48.

Saravanan, R., 1993: *Journal of Atmospheric Sciences*, **50**, 1211–1227.

Schneider, T., 2006: *Annual Review of Earth and Planetary Sciences*, **34**, 655–688.

Scott, R. K., and L. Polvani, 2007: *J. Atmos. Sci.*, **64**, 3158–3176.

Seager, S., L. J. Richardson, B. M. S. Hansen, K. Menou, J. Y.-K. Cho, and D. Deming, 2005: *ApJ*, **632**, 1122–1131.

Showman, A. P., 2007: *J. Atmos. Sci.*, **64**, 3132–3157.

Showman, A. P., and T. Guillot, 2002: *A&A*, **385**, 166–180.

Suarez, M. J., and D. G. Duffy, 1992: *Journal of Atmospheric Sciences*, **49**, 1541–1556.

Sukoriansky, S., N. Dikovskaya, and B. Galperin, 2007: *J. Atmos. Sci.*, in press.

Vallis, G. K., 2006: *Atmospheric and Oceanic Fluid Dynamics: Fundamentals and Large-Scale Circulation*. Cambridge Univ. Press, Cambridge, UK.

Vallis, G. K., and M. E. Maltrud, 1993: *J. Phys. Oceanography*, **23**, 1346–1362.

Vasavada, A. R., and A. P. Showman, 2005: *Reports of Progress in Physics*, **68**, 1935–1996.

Williams, G. P., 1978: *Journal of Atmospheric Sciences*, **35**, 1399–1426.

Williams, G. P., 1979: *Journal of Atmospheric Sciences*, **36**, 932–968.

Williams, G. P., 2003: *Journal of Atmospheric Sciences*, **60**, 1270–1296.

Williams, P. K. G., D. Charbonneau, C. S. Cooper, A. P. Showman, and J. J. Fortney, 2006: *ApJ*, **649**, 1020–1027.

Yoden, S., and M. Yamada, 1993: *Journal of Atmospheric Sciences*, **50**, 631–644.